

## Supplementary Information

# Anomalous Behavior of Nearly-Entire Visible Band Manipulated with Degenerated Image Dipole Array

Lei Zhang,<sup>a</sup> Jiaming Hao,<sup>b</sup> Min Qiu,<sup>c</sup> Said Zouhdi,<sup>d</sup> Joel Kwang Wei Yang<sup>e,f</sup> and Cheng-Wei Qiu<sup>†a</sup>

<sup>a</sup> Department of Electrical and Computer Engineering, National University of Singapore, Singapore 117583, Singapore.

<sup>b</sup> National Laboratory for Infrared Physics, Shanghai Institute of Technical Physics, Chinese Academy of Science, Shanghai 200083, China.

<sup>c</sup> State Key Laboratory of Modern Optical Instrumentation, Department of Optical Engineering, Zhejiang University, Hangzhou 310027, China.

<sup>d</sup> Laboratoire de Génie Electrique de Paris, Paris-Sud University, France.

<sup>e</sup> Institute of Materials Research and Engineering, A\*STAR (Agency for Science, Technology and Research), 3 Research Link, 117602, Singapore.

<sup>f</sup> Engineering Product Development, Singapore University of Technology and Design, 20 Dover Drive, Singapore 138682

<sup>†</sup> Corresponding Author: Cheng-Wei Qiu

Email address: [eleqc@nus.edu.sg](mailto:eleqc@nus.edu.sg)

### 1. Charge distribution

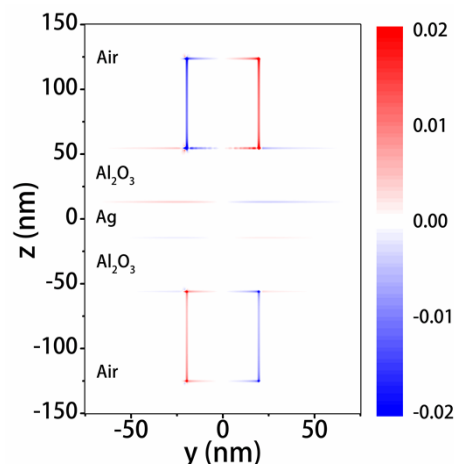


Fig. S1 Charge distribution of one-dimensional nanowire at wavelength  $\lambda = 700$  nm, which supports transmittance as red dashed line shown in Fig. 2d in the main text. It is obvious that dipoles exist on the top and at the bottom. Here  $h = 20$  nm,  $d = 30$  nm,  $t = 50$  nm and  $p_y = 150$  nm.  $L_1 = L_2 = 40$  nm.

### 2. Factors of affecting the bending performance

In order to estimate the phase delay, linear polarized light is normally incident on one-dimensional nanowire array, as shown in Fig. S2a. By enlarging the period of nanowire along y-axis from  $p_y = 150$  nm to 200 nm, larger tunable range of phase is possible with the proposed structure. Coverage of  $2\pi$  phase delay can even be achieved at  $\lambda = 600$  nm with  $p_y = 200$  nm as shown in Fig. S3b. We therefore simulate the bending performance of the structure with  $p_y = 200$  nm,  $L_1 = 10$  nm and  $L_2 = 140$  nm, which is supposed to support phase delay covering  $2\pi$  range at  $\lambda = 600$  nm. As shown in Fig. S3a, the wavefront of structure is even worse than that supported by structure with  $p_y = 150$  nm in the main text. However, the planar feature retains well at  $\lambda = 700$  nm. The main reason can be attributed to the interference between the normal and anomalous transmitted lights. As shown in Fig. S4a, despite of the expected anomalous light, i.e. +1 order, there are energies being distributed to other unexpected orders. For instance, even though the anomalous transmission efficiency is as high as 23% at  $\lambda = 600$  nm, there is 14% energy propagating along the normal direction for structure with  $p_y = 200$  nm. We therefore calculated field distribution of two plane waves. One propagates normally downward with  $E_0 = A_0 \exp(i k_0 z)$ , which corresponds to 0 order, and the other  $E_{+1} = A_{+1} \exp(i(k_0 \sin \theta_{+1} \cdot x + k_0 \cos \theta_{+1} \cdot z))$ , where  $\theta_{+1}$  is set as  $30^\circ$  for +1 order (i.e., the anomalous light).  $A_0$  and  $A_{+1}$  are amplitudes, which can be estimated from Fig. S5. For structure with  $p_y = 200$  nm,  $A_0 = 0.37$  and  $A_{+1} = 0.48$  at  $\lambda = 600$  nm. The little difference in transmitted amplitude will definitely lead to an obvious interference. As a result, the planar feature gets hard to define. In contrast, for structure with  $p_y = 150$  nm,  $A_0 = 0.06$  and  $A_{+1} = 0.54$ . Therefore, the planar feature can be well defined as shown in Fig. S5b. Therefore, one may notice that, although  $2\pi$  phase delay coverage or a constant phase gradient is beneficial for retaining planar feature in anomalous bent wave, it is more important to get rid of other diffraction orders totally. It can also be verified by the field distribution at  $\lambda = 700$  nm, as shown in Fig. S3b. Well-defined wavefront for both refracted and reflected light originates from suppression of other unexpected diffraction order.

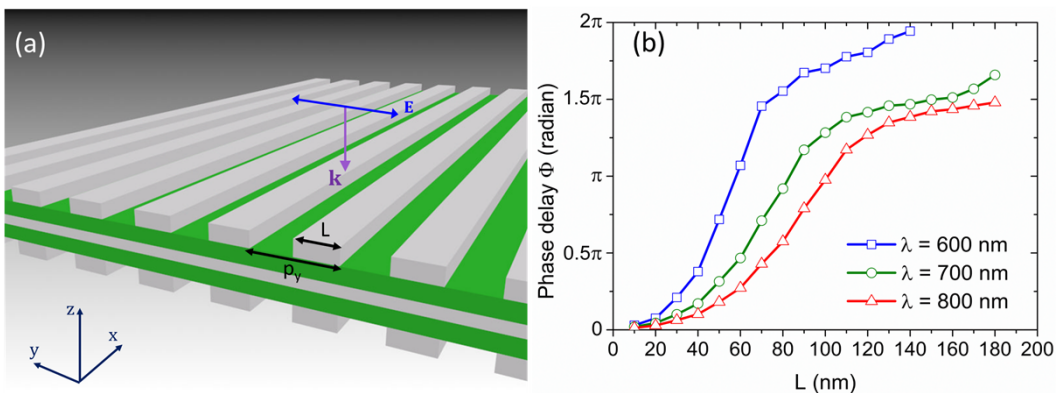


Fig. S2 (a) Schematic structure of one-dimensional nanowire for phase delay estimation and (b) phase delay  $\Phi$  of refracted light versus width of one-dimensional nanowire at wavelength  $\lambda = 600$  nm, 700

nm and 800nm. Here  $h = 20$  nm,  $d = 30$  nm,  $t = 50$  nm and  $p_y = 200$  nm.  $L_1 = L_2 = L$  ranges from 10 nm to 180 nm.

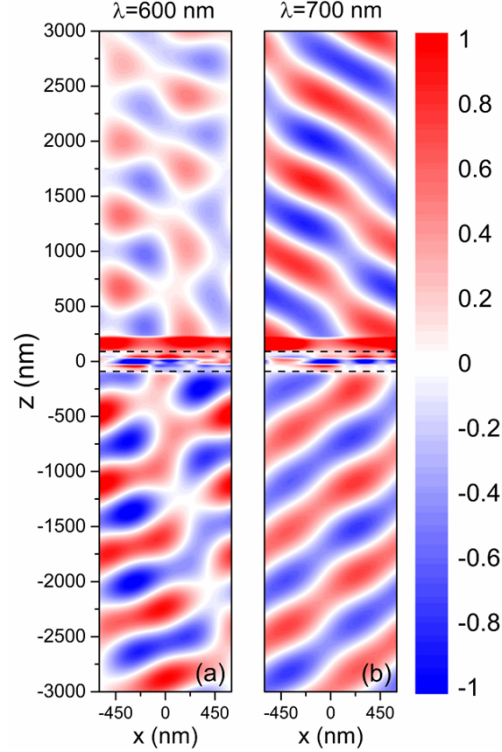


Fig. S3 Electric field distributions of  $E_y$  component at wavelength (a) 600 nm and (b) 700 nm of structure supporting phase delay coverage  $2\pi$  with  $p_y = 200$  nm,  $L_1 = 10$  nm and  $L_2 = 140$  nm. All the simulations are performed at normal incidence. Other parameters are  $h = 20$  nm,  $d = 30$  nm,  $t = 50$  nm and  $p_x = 1200$  nm.

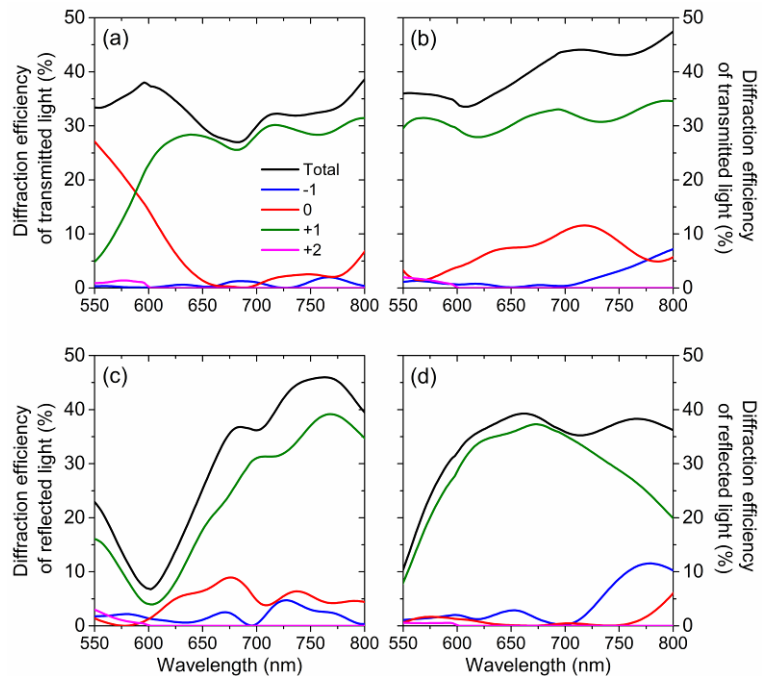


Fig. S4 Diffraction efficiency of transmitted (a) and (b) and reflected (c) and (d) energies against wavelength. (a) and (c) are calculated with  $p_y = 200$  nm while (b) and (d) are calculated with  $p_y = 150$  nm.

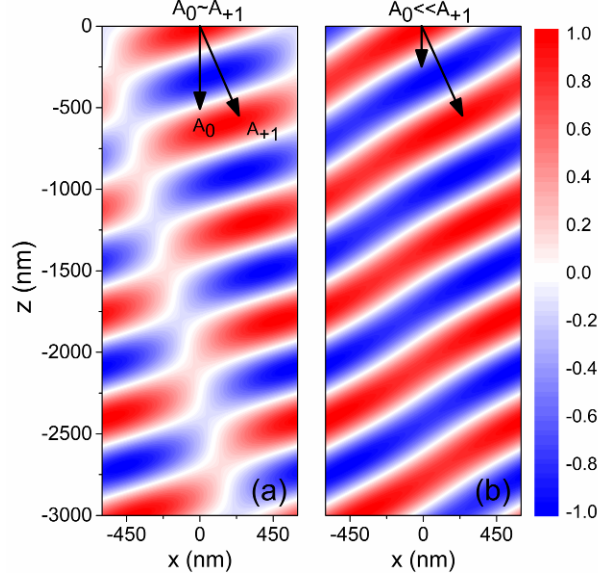


Fig. S5 Interference of 0 and +1 order (anomalous light) for two cases similar to (a)  $p_y = 200$  nm.  $A_0 = 0.37$  and  $A_{+1} = 0.48$  and (b)  $p_y = 150$  nm,  $A_0 = 0.06$  and  $A_{+1} = 0.54$ .

### 3. Phase delay by varying the thickness of $\text{Al}_2\text{O}_3$ layer

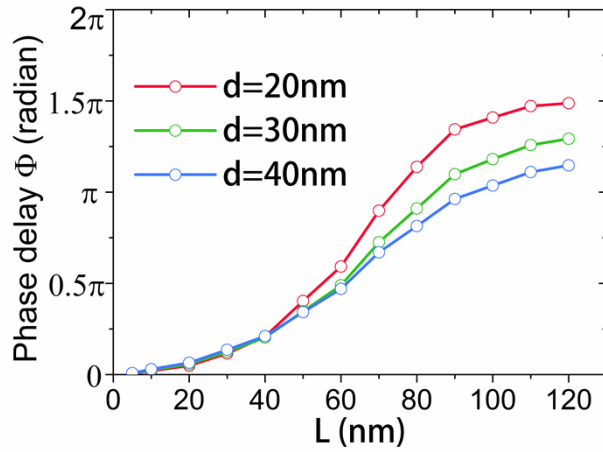


Fig. S6 Phase delay  $\Phi$  of refracted light versus width of one-dimensional nanowire at wavelength  $\lambda = 700$  nm. Here  $h = 20$  nm,  $t = 50$  nm and  $p_y = 150$  nm.  $L_1 = L_2 = L$  ranges from 5 nm to 120 nm.